JOURNAL OF MATERIALS SCIENCE 21 (1986) 2308–2314

Rubber-crumb modified polystyrene

Part 2 *Fracture toughness*

R. P. BURFORD, M. PITTOLO*
School of Chemical Engineering and Industrial Chemistry, University of New South Wales, PO Box 1, Kensington, New South Wales 2033, Australia

The strain energy release rate, G_c, of polystyrene (PS) containing rubber crumb has been examined. It was found that for unmodified crumb, addition of small amounts (5%) leads to 100% increase in G_c. This is attributed to crazing in the PS. However, further addition of crumb leads to reductions in G_c, as the crumb–PS adhesion is low and interfacial failure results. If the crumb is modified with PS its adhesion to the matrix PS increases and internal rupture of the rubber occurs. G_c for these composites increases linearly with crumb loading, and is due to matrix crazing as well as rupture of the rubber phase.

1. Introduction

In a previous paper [1] we described the mechanical properties of polystyrene (PS) containing recycled rubber-crumb fillers. By modifying the crumb with PS, improvements in both breaking stress σ_b and breaking strain ε_b were achieved. In this paper we discuss the fracture energy, G_c, of these composites with particular emphasis on the effect of crumb–matrix adhesion and matrix crazing.

In high-impact polystyrene (HIPS), multiple crazing, which occurs predominantly in the plane stress regime [2], results in a significant increase in the measured strain energy release rate, G_c, or fracture toughness, K_c [3]. In our previous work [1, 4] it was shown that PS-modified crumb was ruptured during crack propagation. As this material is expected to have a G_c higher than that of the PS matrix, its rupture is expected to lead to an increase in composite G_c. This paper attempts to separate the effects of crazing and of rupture of crumb and matrix.

2. Experimental procedure

2.1. Crumb and crumb-filled composite preparation

The preparation of PS sheets containing rubber crumb and grafted rubber crumb has been previously described [1]. In addition, three PS sheets containing a granulated interpenetrating polymer network (IPN) material were prepared. The IPN itself was prepared as follows.

About 25 g of an SBR50 pad was swollen in 75 g styrene monomer containing azobisisobutyronitrile (AIBN) initiator. After allowing 4 days for equilibrium to be reached, the pad was clamped between two stainless steel plates and placed in an oven at 120° C for 24 h. At this stage polymerization was almost complete. The IPN was then removed from the oven and dried under vacuum at 60° C. The solid was then ground in a high-speed mill and incorporated into PS, using a Rheomix internal mixer, as previously described for rubber-crumb filler studies [1, 4].

Microtensile test pieces conforming to ASTM Standard D 1708 were punched from each sheet. These were tested using a cross-head speed of 20 mm min^{-1}.

2.2. Double-torsion tests

The composite fracture toughness was determined by the double-torsion method. Each specimen was 100 mm long, 25 mm wide and 2 mm thick. A central groove 1 mm deep was machined into each specimen before use. The starter crack was inserted by tapping a scalpel blade into the notch to produce a small running crack about 20 to 30 mm long. The specimens were tested at a cross-head speed of 10 mm min^{-1} and G_c was calculated [5] using the equation

$$G_c = \frac{3p^2l^2}{2DB^3B_cE_b} \quad (1)$$

where P = constant load, l, D, B and B_c are specimen dimensions as defined in [5], and E_b is a flexural modulus. The modulus E_b was determined in flexure in separate experiments using ASTM Procedure D790.

2.3. Microscopic examination

The surfaces of the fracture samples were examined using a Nikon stereo microscope and an ISI-100A scanning electron microscope (SEM). Staining procedures are given elsewhere [1].

3. Results and discussion

Three modes of crack propagation were evident, these being "slip–stick", semi-continuous and continuous. Typical load–deflection traces are shown in Fig. 1. G_c was calculated using peak load values for slip–stick behaviour. The mean of the upper and lower values from two specimens is reported and the error bars on graphs give the range.

Slip-stick propagation was found for PS and

Present address: SOLA Optical Australia Pty Ltd, Sherriffs Road, Lonsdale, South Australia 5160, Australia.

0022–2461/86 $03.00 + .12

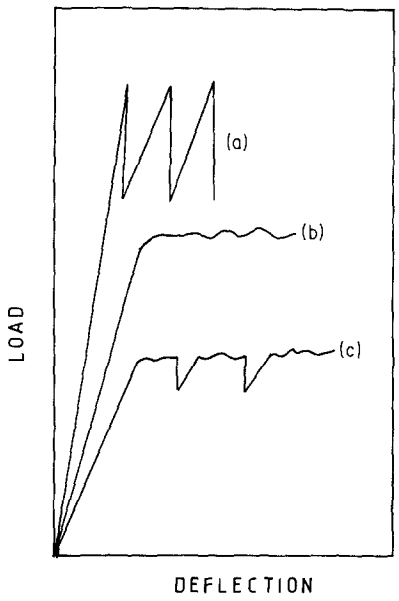

Figure 1 Typical load–deflection traces from double torsion tests: (a) slip–stick; (b) continuous; (c) semi-continuous.

composites containing small amounts of grafted crumb. Continuous propagation was observed for materials containing ungrafted crumb and high levels of grafted crumb. An optical micrograph of the fracture surface of the PS (Fig. 2) shows it to be free of stress-whitening, and it is typical of a brittle fracture, with regularly spaced rib-like markings. Continuous propagation resulted in a highly-reflecting whitened fracture surface. Fig. 3 shows the fracture surface of such a highly whitened specimen (top), compared to that of a non-whitened specimen. The highly iridescent nature of the surface suggests that secondary crazing has occurred below the fracture plane.

3.1. Effect of unmodified crumb

The addition of 5% of all three ungrafted crumbs led to a dramatic increase in G_c. However, as shown in Figs. 4 and 5, further addition reduces G_c. This trend is similar to that found by Nikpur and Williams [6] for the K_c of HIPS tested at low cross-head speeds. They concluded that the addition of a small amount of rubber led to complete utilization of the crazing potential of the rubber. Further increase of the rubber content led to reduced K_c due to the reduced σ_y. These composites do not yield and so the reduction in G_c must be attributed to some other process.

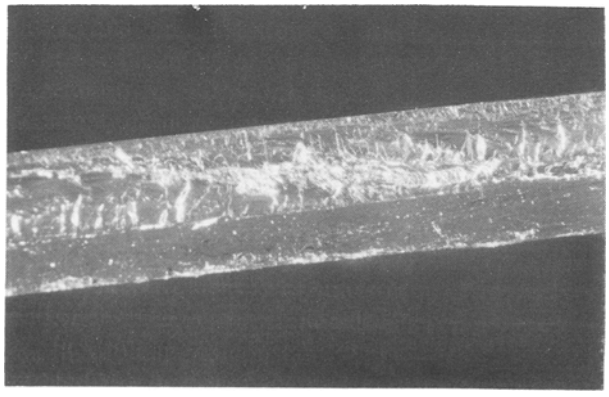

Figure 2 Optical micrograph of PS fracture surface (× 10).

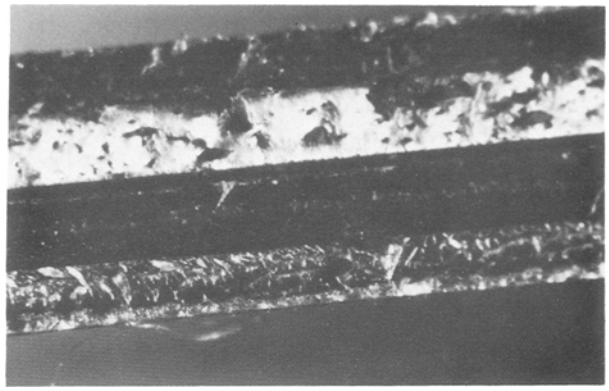

Figure 3 Optical micrograph of stress-whitened and non-whitened composite (× 10).

Kendall [7] developed a model which relates composite G_c to the fracture toughness of matrix, G_m, and filler, G_f. G_f may be the G_c of the filler or the adhesive energy, G_a, of the filler–matrix interface. He developed the equation

$$G_c = G_m(1 - k\phi_f) + nk\phi_f G_f \qquad (2)$$

where ϕ_f is the volume fraction of filler. The parameter n is the ratio of filler cross-sectional area to the area exposed during rupture. The constant k allows for the increase in filler concentration of the fracture surface, which may arise through crack deviation.

For composites containing BR50, interfacial adhesion was negligible, so G_f was zero and a value $n = 2$ was assumed. The value of k was thus calculated to be 2.6, which is unrealistically high. Also shown in Fig. 4 are the values of G_c predicted using a minimum-area model (broken line) assuming a matrix $G_c = 2\,\mathrm{kJ\,m^{-2}}$ calculated from the equation [8]

$$G_c = G_m(1 - 1.21\phi_f^{2/3}) \qquad (3)$$

This model assumes that the crumb particles act as voids and that a propagating crack proceeds along a minimum-area path (i.e. the path of least resistance). The predicted and experimental values are in close agreement.

An electron micrograph of the fracture surface

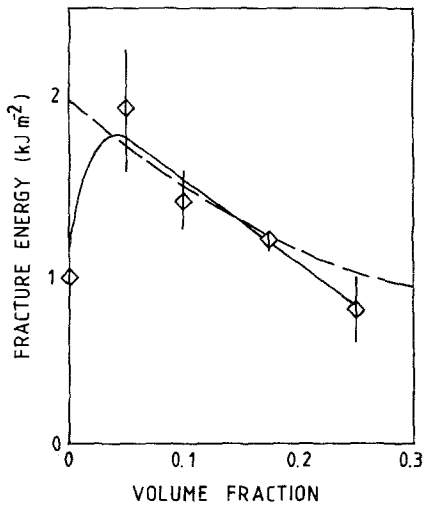

Figure 4 Fracture energy of composite containing modified BR50 crumb.

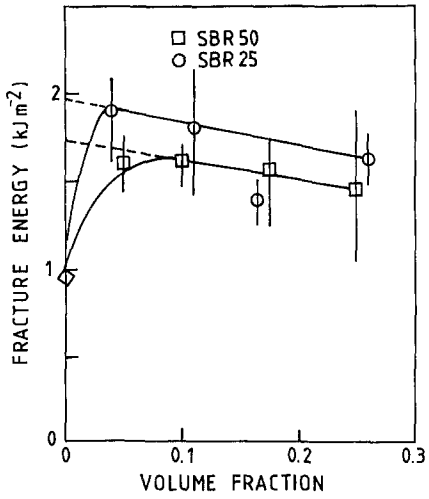

Figure 5 Fracture energy of composites containing modified SBR50 crumb: (○) SBR25, (□) SBR50.

(Fig. 6) indicates that interfacial failure has occurred, as the cavity has an angular shape corresponding to the extracted filler particle. In addition there appears to be stained craze-like porous material in the matrix. There is no evidence of staining in the cavities from which the filler has been pulled. This contrasts strongly with the appearance of the PS fracture surface (Fig. 7) where porous zones are absent. There are, however, rib-like structures similar in appearance to "mackerel" markings. Fig. 8 shows the fracture surface of the composite containing 5% BR50. Staining in the matrix around the crumb particles may result from the low crumb-to-PS adhesion, thus allowing rapid diffusion of OsO_4 into the crazed matrix. These regions appear, at higher magnification, to have a layered structure which may result from crack growth through a craze bundle.

These micrographs suggests that the improvement in G_c of these composites results from crazing of the matrix. The reduction in G_c at higher crumb loadings results from the low G_a.

The data for composites containing crumbs SBR25 and SBR50 were also fitted to the Kendall model. Again $n = 2$ was assumed and, as interfacial failure occurred, G_f was taken as G_a (which was found to be $0.37\,kJ\,m^{-2}$). From the lines of best fit, values of k were found to be 1.2 and 0.89 for SBR25- and SBR50-filled composites, respectively. The values are close to the expected value of 1 (given no crack deviation). These calculations do not allow for energy dissipation in stretching the crumb particles before "pull-out", although the close agreement with the expected results suggests that this contribution is small.

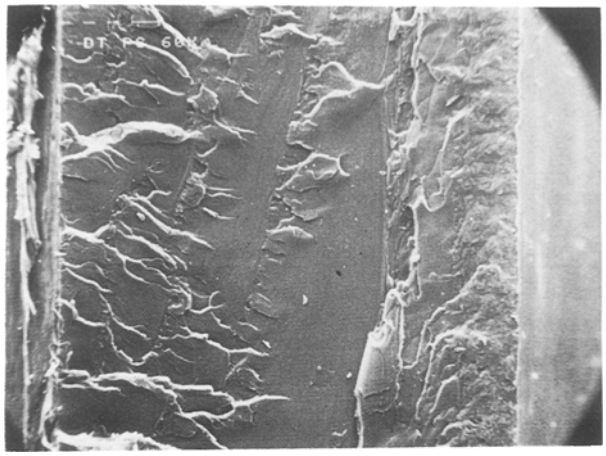

Figure 7 Fracture surface of PS (× 40).

The fracture surfaces of these composites were similar in appearance to those containing BR50, and so the improvement in G_c is similarly attributed to matrix crazing.

The previous calculations assume that the matrix G_c, G_m, is equal to the intercept of the line of best fit. This implies that the addition of a small amount of crumb is sufficient to fully utilize the crazing potential of the matrix, and that further addition of crumb does not alter G_m. G_m for composites containing crumb BR50 and SRB25 were found to be about $2\,kJ\,m^{-2}$. These crumbs also have similar moduli. Composites containing SBR50, which has a higher modulus, have a slightly lower G_m ($1.67\,kJ\,m^{-2}$), indicating that the crumb modulus may affect the degree of crazing in the PS. Increasing the modulus of the crumb decreases the stress concentrations in the matrix and hence the crazing. The increased curvature of the G_c–ϕ_f curve for SBR50 crumbs may indicate that complete utilization of the crazing potential of the matrix requires a higher crumb loading.

Figure 6 Fracture surface of composite containing 25% SBR50. (× 221).

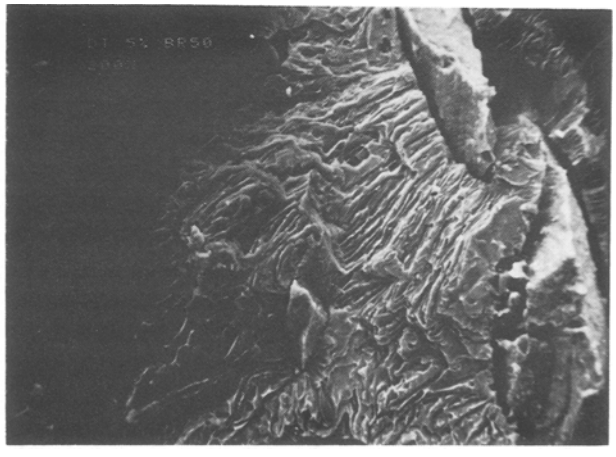

Figure 8 Fracture surface of composite containing 5% BR50 (× 134).

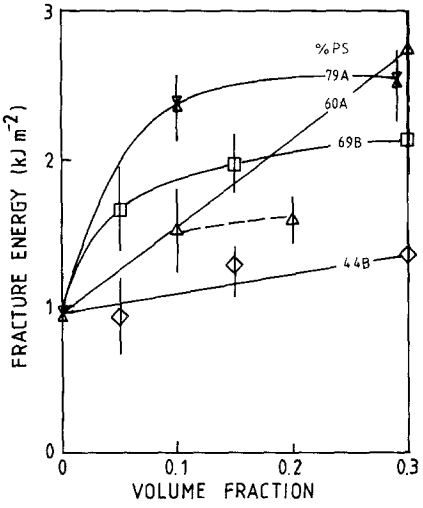

Figure 9 Fracture energy of PS containing BR50 as a function of crumb volume fraction: (◇) 44B, (△) 60A, (□) 69B, (⧖) 79A.

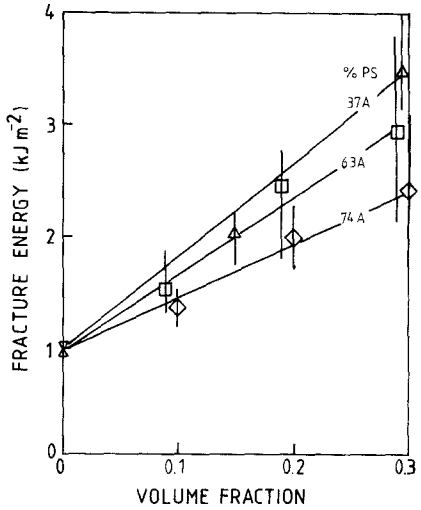

Figure 10 Fracture energy of PS containing SBR50 and SBR25 crumbs as a function of volume fraction: (△) 37A, (□) 63A, (◇) 74A.

3.2. Effect of PS-modified crumb

Values of G_c determined for composites containing PS-modified crumb are shown in Figs. 9 and 10. It can be seen that all composites have G_c values which increase continuously up to $\phi_f = 0.30$. The results for modified BR50 crumb show two different relationships.

Composites containing BR50/44B and BR50/79A had load–deflection traces typical of slip–stick or semi-continuous crack propagation. Slip–stick behaviour predominated at low ϕ_f. Stress-whitening on the fracture surface was also limited, but increased with increasing ϕ_f. These composites have a linear G_c–ϕ_f relationship (although there is some scatter in the results for BR50/79A). Composites containing BR50/69 and BR50/60A exhibited continuous, steady crack growth at all values of ϕ_f, and the fracture surfaces were completely stress-whitened. These composites also have a non-linear G_c–ϕ_f relationship, with G_c tending to level off at $\phi_f \simeq 0.15$.

All composites tested containing modified SBR50 showed linear G_c–ϕ_f curves. They also underwent slip–stick or semi-continuous crack growth, and stress-whitening increased with ϕ_f. The fracture surfaces of composites containing SBR50/63A were shown previously in Fig. 3 (top layer $\phi_f = 0.30$, bottom layer $\phi_f = 0.10$).

The fracture surface of the composite containing 10% SBR50/63A (Fig. 11a) was shown by SEM to be very similar in appearance to that of the PS matrix. Closer examination (Fig. 11b) reveals regions, usually near ruptured rubber particles, which have a drawn, layered appearance, suggesting multiple crazing. At high ϕ_f the surface becomes much rougher and bears little resemblance to that of PS (Fig. 12).

The increase in G_c of these composites, above that of PS, arises from two sources. As all composites exhibit internal filler rupture, the expected high G_c or τ of the ber phase must contribute to the composite G_c (where τ is the tear energy). The second source of improvement is induced crazing of the matrix. This is evident from the iridescent appearance of the fracture surface and the evidence of plastic deformation from electron micrographs.

In composites which have non-linear relationships between G_c and ϕ_f, it appears that addition of the crumb causes a dramatic increase in matrix crazing. This is similar to the behaviour of composites containing untreated crumb. However, G_c is not reduced by further crumb addition, as the rubber particles must be ruptured during fracture and so contribute to G_c.

For composites having linear G_c–ϕ_f relationships, stress-whitening increases with ϕ_f. The application of

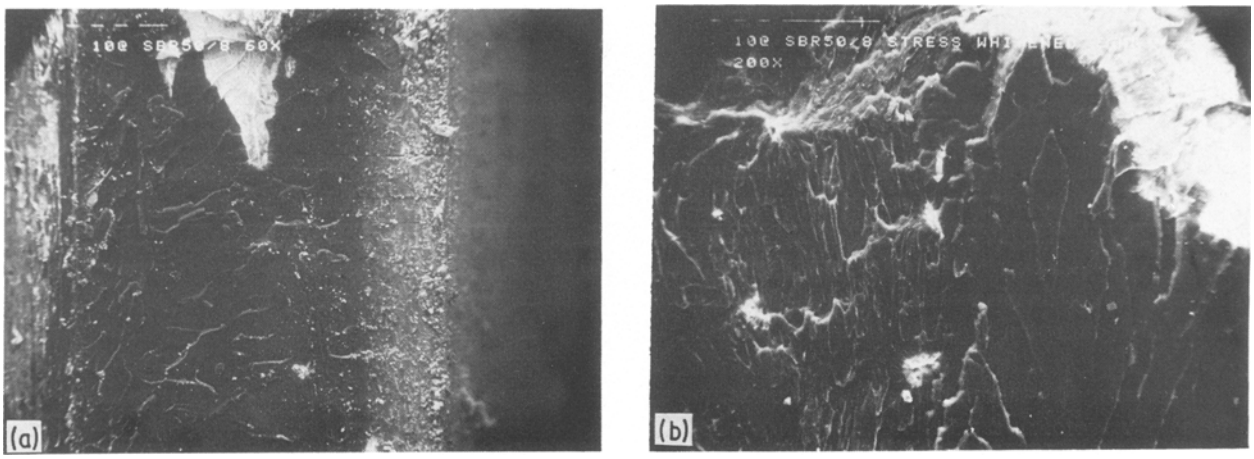

Figure 11 Fracture surface of composite containing 10% SBR50/63A: (a) × 40, (b) stress-whitened zone (× 134).

TABLE I Calculated values of crumb fracture energy G_f

Crumb	PS content (%)	G_f (kJ m^{-2})
SBR50/37A	37	9.85
SBR50/63A	63	7.77
SBR50/74A	74	5.93

TABLE II Mechanical properties of IPN (SBR50/70PS)

Property	IPN	HIPS
Modulus (MPa)	621 ± 36	1532 ± 98
σ_y (MPa)	26.13 ± 0.65	27.23 ± 0.78
σ_b (MPa)	23.97 ± 0.39	23.09 ± 0.74
ε_b (%)	34 ± 12	6.48 ± 1.57

the Kendall model [7] to G_c values of composites containing modified SBR50 crumb gives the apparent value of G_f (filler G_c). Both n and k are assumed to be unity. The values of G_f thus calculated have contributions from filler rupture and matrix crazing, and are tabulated in Table I. These results show that the improvement in composite G_c increases as the PS content of the crumb decreases. Decreasing the PS content will reduce the modulus of the rubber phase and hence increase its ability to initiate crazing.

The SBR50 compound has a tear energy of about 50 kJ m^{-2}, while G_c of PS is about 1 kJ m^{-2}. Assuming synergism to be absent, it is expected that the G_c of the rubber phase will decrease with increasing PS content. Thus the contribution to composite G_c from rupture of the rubber phase will decrease.

The decrease in G_f with increasing rubber-phase PS content is the result of decreases in both matrix crazing and rubber-phase G_c.

3.3. Optical microscopy of crack propagation

The mode of crack propagation was studied using a crack-opening device mounted under the optical microscope. About 1 g of crumb (either treated or untreated) was dispersed in 60 g of PS. The composite was then compression-moulded and double-torsion test pieces were shaped from the sheet. These specimens were found to be ideal for this study as the advancing crack was restricted to the central groove.

When unmodified SBR50 was used as the filler, some crack bridging was evident as shown in Fig. 13. However, interfacial failure still occurred, as reflected by particles protruding from the fracture surface.

Fig. 14 shows a particle of modified SBR50 crumb (marked "A") bridging a crack. However, other particles in the vicinity (marked "B") ruptured during crack-tip advancement. On further straining the bridging particle also ruptures. The difference in behaviour of these particles is believed to result in the different appearance of the ruptured particles seen on the fracture surfaces of tensile specimens.

3.4. Model studies using ground IPN

Styrene-treated crumbs constitute semi-IPNs, being cross-linked elastomers interpenetrated with linear polystyrene. After a number of attempts it was found that by using the conditions and procedures given in Section 2, macroscopically uniform IPNs could be prepared. The IPN used in this work consisted of SBR50 containing 71% PS.

The mechanical properties of the IPN are given in Table II. The IPN has similar σ_b and σ_y to that of the HIPS sample, but ε_b was greater. The large variation in ε_b is probably due to small flaws introduced when the tensile dumb-bells were punched from the sheet.

By grinding the IPN and using it as a filler in PS it was hoped that the relationship between composite G_c and that of the filler could be studied and the contribution to composite G_c from crazing evaluated. To achieve this, G_c for the IPN must be determined. In the composite the IPN will be restrained by the surrounding matrix and so its G_c would be expected to approach the plane-strain value.

The problems associated with determining the plane-strain K_c of tough plastics such as HIPS were overcome by Yap *et al.* [9] who used single-edge notched (SEN) specimens which are more aptly described as face-notched. They recommended that the specimen thickness (across the face) should be at least $7.5(K_c/\sigma_y)^2$, but made no comment on what the width should be although K_c was the same for specimens of width 4.7 and 9.4 mm [10].

It was decided that 40 mm-thick SEN specimens were suitable for determining K_c for the IPN where only limited material was available. Each specimen was 120 mm long and 3.6 mm "wide", the "width"

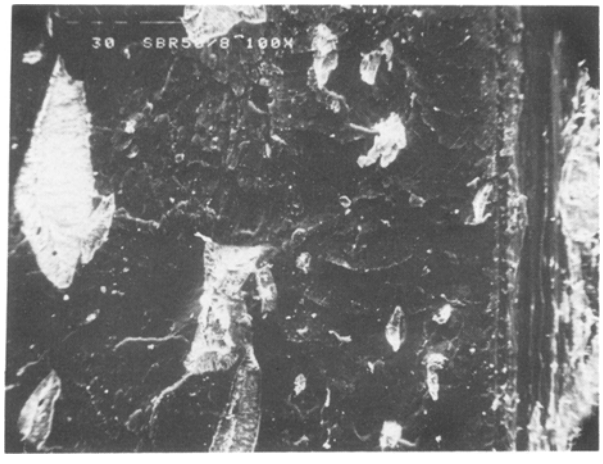

Figure 12 Fracture surface of composite containing 30% SBR50/63A (× 67).

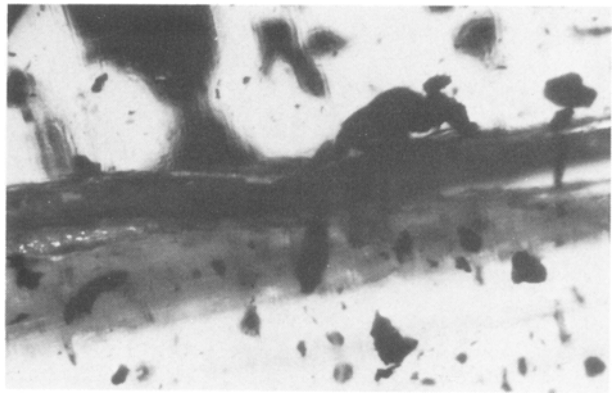

Figure 13 Interfacial failure in composite containing SBR50 (× 10).

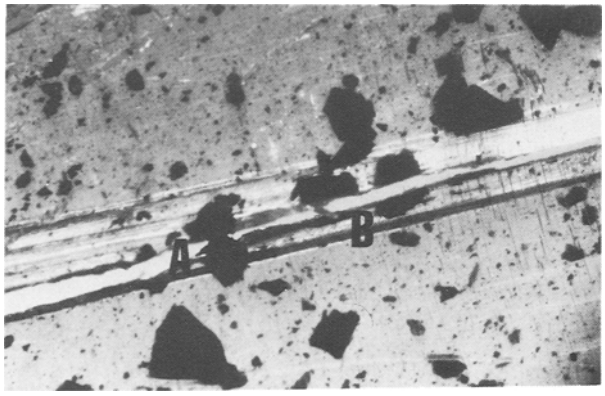

Figure 14 Crack in composite containing PS-modified crumb, showing crack bridging and particle rupture (× 6).

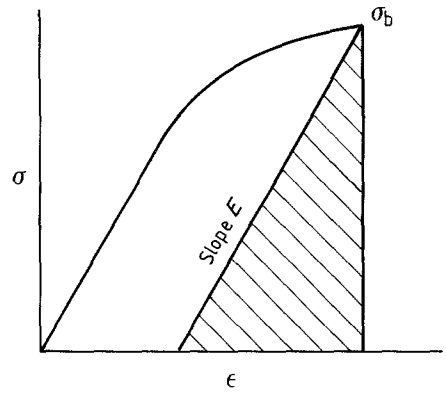

Figure 16 Difference in energy associated with linear elastic fracture mechanics assumption (shaded part) compared with actual stress–strain behaviour.

being limited by the sheet thickness. The value of K_c thus determined was $1.34 \pm 0.24\,MN\,m^{-3/2}$. The specimen thickness was about twice the lower limit recommended by Yap *et al.* [9], suggesting that this value was close to the plane-strain value. However, there was some non-linearity in the load–deflection traces at small crack lengths, indicating subcritical crack growth. The value of K_c, which corresponds to a G_c of $2.99\,kJ\,m^{-2}$, may thus overestimate the plane-strain value.

The IPN was ground in a cryogenic mill and sieved to two particle-size ranges (i.e. less than 1 mm, and 2 to 1 mm) before use. PS composites containing the smaller particle-size crumb were prepared with ϕ_f from 0.1 to 0.5. One composite with $\phi_f = 0.30$ was prepared from the larger crumb. Double-torsion tests were carried out to determine G_c, and the results are presented in Fig. 15. The solid line represents the predicted value using Equation 1 (the Kendall model [7]) assuming $n = k = 1$.

Although G_c is linearly related to ϕ_f, it is well above that predicted as a result of either matrix crazing or underestimation of G_f. Given the stress-whitened appearance of the fracture surface, the former is the most likely explanation. The apparent value of G_f was calculated from the line of best fit and found to be $5.11\,kJ\,m^{-2}$. The contribution to toughening from crazing is thus found to be approximately 40%.

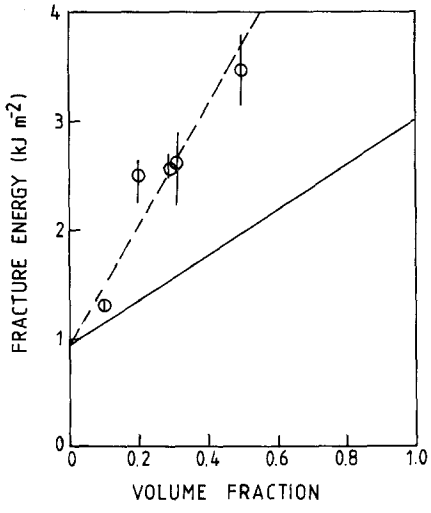

Figure 15 Fracture energy of composites containing ground IPN material, as a function of volume fraction.

It is also seen that the composite containing the large particle size crumb has an equivalent G_c to that containing the small crumb at the same ϕ_f. This is in good agreement with Equation 1, which has no particle size term, and indicates that craze initiation is not dependent on particle size. Such a dependence might have been expected, as the particles act as craze initiators and decreasing the particle size increases their number at a given value of ϕ_f.

3.5. Relationship between breaking stress and strain energy release rate

In thermoplastics, where crazing and shear yielding can occur, there is considerable difficulty in correlating strain energy release rate, G_c, and breaking stress σ_b. For these reasons, little has been published except for rubber fracture. However, some comments are relevant.

When flaw-size (c) calculations are made using

$$c = \frac{(2EG_c)^{1/2}}{\pi\sigma_b} \quad (4)$$

(which assumes that the energy available for crack propagation is given by the shaded area in Fig. 16), c for PS was typically found to be about 0.6 mm. For samples containing crumb or grafted crumb, c varied between 0.9 and 2.0 mm, with no apparent trend. The significance of these results is unclear.

In Kinlock and Young's monograph [11], a value of c of 0.5 mm for PS is reported and this corresponds closely to the craze length before fracture. For filled PS, our values may represent the size of filler or filler plus induced craze. For epoxy resins containing 10 μm diameter silica filler, c was calculated to be about 200 μm [11], although no observable discontinuity of this magnitude was found on the fracture surface.

Another factor to be considered is that the conditions under which σ_b was determined were vastly different to those under which G_c was determined. Perhaps a better correlation between G_c and σ_b could be obtained if SEN tests were used to determine K_c. In this regard a more detailed study of crumb particle size would be particularly appropriate and useful. Variations in E also affect c, so that although G_c may

increase with crumb loading the resultant variation in c is affected by the decrease in both $E^{1/2}$ and σ_b.

4. Conclusions

G_c for PS increases by up to 100% on addition of small amounts (5%) of ungrafted crumb, and this has been attributed to crazing in the matrix. Further addition leads to a reduction in G_c due to low interfacial adhesion. When grafted crumb is added G_c increases continuously with ϕ_f. This is attributed to matrix crazing in addition to a large contribution from rupture of the rubber phase, which has a higher G_c than the PS matrix. The fact that crazing also contributes to composite G_c is evident from the morphology of the fracture surface. Further confirmation came from model studies, where composite G_c was much greater than the value predicted by a simple averaging model.

References

1. M. PITTOLO and R. P. BURFORD, *J. Mater. Sci.* **21** (1986) 1769.
2. M. PARVIN and J. G. WILLIAMS, *ibid.* **11** (1976) 2045.
3. C. B. BUCKNALL, "Toughened Plastics" (Applied Science, London, 1977).
4. M. PITTOLO and R. P. BURFORD, *Rubber Chem. Technol.* **58** (1985) 97.
5. J. G. WILLIAMS, *Adv. Polym. Sci.* **27** (1978) 67.
6. K. NIKPUR and J. A. WILLIAMS, *J. Mater. Sci.* **14** (1979) 467.
7. K. KENDALL, *Br. Polym. J.* **10** (1978) 35.
8. O. ISHAI and L. J. COHEN, *J. Compos. Mater.* **2** (1968) 302.
9. O. F. YAP, Y. W. MAI and B. COTTERELL, *J. Mater. Sci.* **18** (1983) 657.
10. Y. W. MAI, private communication (1984).
11. A. J. KINLOCH and R. Y. YOUNG, "Fracture Behaviour of Polymers" (Applied Science, London, 1983) Ch. 7.

Received 29 March
and accepted 10 September 1985